Sub-Poissonian light from a laser with an injected signal

Márcia T. Fontenelle
Departamento de Física, Pontifícia Universidade Católica do Rio de Janeiro, Caixa Postal 38071, 22452-970 Rio de Janeiro, Rio de Janeiro, Brazil

L. Davidovich
Instituto de Física, Universidade Federal do Rio de Janeiro, Caixa Postal 68528, 21945-970 Rio de Janeiro, Rio de Janeiro, Brazil
(Received 5 August 1994)

We show that the injection of an external field in a laser helps to improve amplitude squeezing and sub-Poissonian light generation close to threshold, but spoils quantum noise reduction for very high pumping rates. A general nonlinear theory is developed for the resonant case (no detunings), without any assumption on the relative magnitudes of field and atomic decay constants, thus encompassing a large class of lasers. Several possible pumping schemes are accommodated, ranging from regular to Poissonian. We carry out a detailed stability analysis of the general equations of motion, relating it to the noise-reduction problem. Both the photon-number variance inside the cavity and the homodyne spectra of the output are discussed.

PACS number(s): 42.50.Dv, 42.50.Lc, 42.55.−f, 42.50.Ne

I. INTRODUCTION

The search for bright sources of light exhibiting either subshot noise or quadrature squeezing has stimulated a strong renewal of interest in basic laser theory. In fact, it has been shown that careful consideration of the pumping mechanism leads to a reformulation of the theory for non-Poissonian pumping and to new possibilities of sub-Poissonian light generation [1,2]. Correlated emission schemes, in which the lasing atoms are initially prepared in a coherent superposition of the resonant states, lead to amplitude squeezing [3] or, in the special case of two-photon lasers, to phase squeezing [4]. Closed systems of states lead to dynamic pump-noise suppression through the recycling of the active laser electron from the lower to the upper laser level via a multistep process [5]. On the other hand, open-system lasers operating in regimes where the atomic variables behave in a nonadiabatic way may also emit sub-Poissonian light, even when no attempt is made to regularize the pumping [6]. This is true even in the rate-equation regime, as long as the field decays in a time scale comparable to that for the upper atomic lasing level [6].

In this paper, we discuss in detail the spectral properties of a laser with an injected signal. This system has been the object of many discussions in the literature, especially in regard to its classical dynamics, since Spencer and Lamb [7] showed that the output intensity may exhibit oscillatory behavior. The chaotic regime has been studied in detail by many authors [8]. Our treatment does not make any assumption about the relative magnitudes of the atomic and field decay constants and it is therefore applicable to a wide variety of laser systems. We consider here the resonant case: the effect of detunings between the injected field, the atoms, and the cavity mode will be considered elsewhere. We are led to two main conclusions: as compared with the situation in which there is no injected signal, there is an enhancement of squeezed-state production for operation not far above threshold and a lowering of the minimum pumping rate necessary for a certain degree of squeezing to appear. In particular, we show that a Poisson-pumped laser may produce sub-Poissonian light, with up to 50% of noise reduction in the output field. Although reminiscent of the noise quenching found in Ref. [6], the introduction of an external coherent signal leads to the possibility of getting sub-Poissonian output in a region much closer to the oscillation threshold than the one found in [6].

We also undertake an analysis of the stability of this system, discussing the connection between some of the main features of the fluctuations spectra and the positions of the roots of the characteristic polynomial obtained in the stability analysis. Two of the main consequences of the nonlinearities in the atom-field interaction, namely, the production of sub-Poissonian light and the appearance of instabilities, are thus related.

Our model is defined in Sec. II, where the Heisenberg-Langevin equations of motion for the field and atomic operators are derived. By choosing a normal-ordered representation, equivalent stochastic c-number equations are written in Sec. III. They allow us to discuss the properties of the steady state, and to obtain the quantum fluctuations around it. In the same section we calculate the spectra of amplitude and phase quadrature components of the cavity-field fluctuations. The spectra of fluctuations for the output field are calculated in Sec. IV and our conclusions are summarized in Sec. V. In the Appendix we make a stability analysis of the model here considered, making sure that the calculated spectra indeed correspond to stable regions. The results obtained in the Appendix are also useful to the discussion made in Sec. IV on the connection between the spectra of fluctuations and the instability thresholds.

II. HEISENBERG-LANGEVIN APPROACH

We consider a system of homogeneously broadened two-level atoms in resonant interaction with a mode of the electromagnetic field in a ring cavity of length L and volume V. The field in the cavity is damped at rate $\gamma/2$, due to both internal losses and transmission through the mirrors, and driven by an external coherent optical signal $\lambda(t)$, also resonant with the cavity mode. We neglect here the phase diffusion of the injected signal since it has no influence whatsoever on the amplitude squeezing effects considered in this paper.

In the electric dipole and rotating-wave approximations, the Hamiltonian describing this system can be written as

$$H = \hbar\Omega a^\dagger a + \sum_j \left(E_a \sigma_a^j + E_b \sigma_b^j\right) + \hbar g \sum_j \Theta(t - t_j)\left(a^\dagger \sigma_j e^{-i\vec{k}\cdot\vec{r}_j} + \sigma_j^\dagger a e^{i\vec{k}\cdot\vec{r}_j}\right) + i\hbar\frac{\gamma}{2}\left(\lambda e^{-i\Omega t}a^\dagger - \lambda^* e^{i\Omega t}a\right), \quad (1)$$

where $a^\dagger$ and a are the photon creation and annihilation operators, σ_j is the polarization operator for the jth atom, and σ_a^j and σ_b^j are the upper- and lower-level population operators, respectively, for the jth atom. E_a and E_b are the energies of the atomic upper and lower levels, respectively, with $E_a - E_b = \hbar\Omega$. $\Theta(t)$ is the step function, which guarantees that the jth atom starts interacting with the field (either because it is pumped to a resonant level or because it enters the cavity) at the instant t_j. The constant g corresponds to the electric dipole coupling between the two-level atoms and the field, while $\vec{r}_j$ is the position of the nucleus of atom j.

We follow closely the method used by Kolobov *et al.* [6]. The interaction between the atoms and the field is described by a set of Heisenberg-Langevin equations of motion, obtained from (1) by adding to the corresponding Heisenberg equations of motion the damping terms and respective fluctuation forces associated with the coupling to the atomic and field reservoirs [9,10]:

$$\dot{a}(t) = -i\Omega a(t) - ig\sum_j \Theta(t - t_j)\sigma_j(t)e^{-i\vec{k}\cdot\vec{r}_j} - \frac{\gamma}{2}a(t) + \frac{\gamma}{2}\lambda e^{-i\Omega t} + F_\gamma(t), \quad (2a)$$

$$\dot{\sigma}_j(t) = -i\Omega\sigma_j(t) + ig\Theta(t - t_j)\left[\sigma_a^j(t) - \sigma_b^j(t)\right]e^{i\vec{k}\cdot\vec{r}_j}a(t) - \Gamma\sigma_j(t) + f_\sigma^j(t), \quad (2b)$$

$$\dot{\sigma}_a^j(t) = ig\Theta(t - t_j)\left[a^\dagger(t)\sigma_j(t)e^{-i\vec{k}\cdot\vec{r}_j} - \sigma_j^\dagger(t)a(t)e^{i\vec{k}\cdot\vec{r}_j}\right] - (\Gamma_a + \Gamma_a')\sigma_a^j(t) + f_a^j(t), \quad (2c)$$

$$\dot{\sigma}_b^j(t) = -ig\Theta(t - t_j)\left[a^\dagger(t)\sigma_j(t)e^{-i\vec{k}\cdot\vec{r}_j} - \sigma_j^\dagger(t)a(t)e^{i\vec{k}\cdot\vec{r}_j}\right] - \Gamma_b\sigma_b^j(t) + \Gamma_a'\sigma_a^j(t) + f_b^j(t), \quad (2d)$$

where Γ, Γ_a, Γ_b, and Γ_a' are atomic polarization and population decay rates. Note that Γ_a' refers to the nonradiative decay from state a to state b, while Γ_a and Γ_b refer to the decay of levels a and b towards other levels.

The correlation functions of the field Langevin noise operators $F_\gamma(t)$ are calculated assuming that the field interacts with a heat bath, producing [9,10]

$$\langle F_\gamma^\dagger(t)F_\gamma(t')\rangle = \overline{n}_T\frac{\gamma}{2}\delta(t - t'), \quad (3a)$$

$$\langle F_\gamma(t)F_\gamma^\dagger(t')\rangle = (\overline{n}_T + 1)\frac{\gamma}{2}\delta(t - t'), \quad (3b)$$

$$\langle F_\gamma(t)F_\gamma(t')\rangle = 0, \quad (3c)$$

where $\overline{n}_T$ is the average number of thermal photons in the laser cavity. We assume for simplicity that the heat reservoir is at zero temperature, so that $\overline{n}_T = 0$. The generalization of our results to nonzero temperatures is straightforward.

The correlation functions of the atomic Langevin noise operators are obtained directly from the generalized Einstein relations [9,10], so that, if

$$\frac{d}{dt}A_\mu = D_\mu + f_\mu(t)$$

with D_μ being an arbitrary function of the operators A_ν, and

$$\langle f_\mu(t)f_\nu(t')\rangle = 2D_{\mu\nu}\,\delta(t - t'),$$

then

$$2D_{\mu\nu} = -\langle D_\mu A_\nu\rangle - \langle A_\mu D_\nu\rangle + \frac{d}{dt}\langle A_\mu A_\nu\rangle.$$

In this way, the following nonvanishing correlation functions are obtained:

$$\langle f_\sigma^{\dagger j}(t)f_\sigma^j(t')\rangle = (2\Gamma - \Gamma_a - \Gamma_a')\langle\sigma_a^j(t)\rangle\,\delta(t - t'), \quad (4a)$$

$$\langle f_\sigma^j(t)f_\sigma^{\dagger j}(t')\rangle = \left[(2\Gamma - \Gamma_b)\langle\sigma_b^j(t)\rangle + \Gamma_a'\langle\sigma_a^j(t)\rangle\right]\delta(t - t'), \quad (4b)$$

$$\langle f_\sigma^j(t)f_a^j(t')\rangle = (\Gamma_a + \Gamma_a')\langle\sigma^j(t)\rangle\,\delta(t - t'), \quad (4c)$$

$$\langle f_\sigma^j(t)f_b^j(t')\rangle = -\Gamma_a'\langle\sigma^j(t)\rangle\,\delta(t - t'), \quad (4d)$$

$$\langle f_\sigma^{\dagger j}(t)f_b^j(t')\rangle = \Gamma_b\langle\sigma_j^\dagger(t)\rangle\,\delta(t - t'), \quad (4e)$$

$$\langle f_a^j(t)f_a^j(t')\rangle = (\Gamma_a + \Gamma_a')\langle\sigma_a^j(t)\rangle\,\delta(t - t'), \quad (4f)$$

$$\langle f_a^j(t)f_b^j(t')\rangle = -\Gamma_a'\langle\sigma_a^j(t)\rangle\,\delta(t - t'), \quad (4g)$$

$$\langle f_b^j(t)f_b^j(t')\rangle = \left[\Gamma_b\langle\sigma_b^j(t)\rangle + \Gamma_a'\langle\sigma_a^j(t)\rangle\right]\delta(t - t'). \quad (4h)$$

As usual, we define the slowly varying field and polarization operators in the frame rotating at frequency Ω:

$$\tilde{a}(t) = e^{i\Omega t}a(t), \quad \tilde{\sigma}_j(t) = e^{i\Omega t}\sigma_j(t).$$

The corresponding Langevin equations are then identical to those for $a(t)$ and $\sigma_j(t)$ with the difference that terms proportional to Ω disappear, as well as the explicit time dependence in the term proportional to λ, viz., the exponential $e^{-i\Omega t}$. In the following we drop the tilde on the operators, keeping in mind that from now on all operators are defined in the rotating frame.

We are interested in the behavior of macroscopic

atomic operators, obtained by adding up the individual atomic operators, taking into account the corresponding injection times,

$$M(t) = -i\sum_j \Theta(t-t_j)\sigma_j(t)e^{-i\vec{k}\cdot\vec{r}_j}, \tag{5a}$$

$$N_a(t) = \sum_j \Theta(t-t_j)\sigma_a^j(t), \tag{5b}$$

$$N_b(t) = \sum_j \Theta(t-t_j)\sigma_b^j(t). \tag{5c}$$

The operator $M(t)$ represents the macroscopic atomic polarization, while $N_a(t)$ and $N_b(t)$ represent the macroscopic populations of the upper and lower levels, respectively. One should note that these operators depend on the distribution of injection times. Thus, as noted elsewhere [2,6], average values or correlation functions involving these macroscopic operators should include not only the quantum-mechanical average, but also the classical average over the statistics of the injection times t_j. This last average depends on the nature of the pumping process, and it becomes relevant when the equations for the macroscopic operators are written down. The Langevin equations for the macroscopic atomic operators are found by differentiating Eqs. (5) and substituting Eqs. (2b)–(2d) for the time derivatives of the individual atomic operators. Thus, for the operator $N_a(t)$ we obtain

$$\begin{aligned}\dot{N}_a(t) &= \sum_j [\delta(t-t_j)\sigma_a^j(t) + \Theta(t-t_j)\dot{\sigma}_a^j(t)] \\ &= \sum_j \delta(t-t_j)\sigma_a^j(t_j) - (\Gamma_a+\Gamma'_a)N_a(t) \\ &\quad -g[a^\dagger(t)M(t) + M^\dagger(t)a(t)] \\ &\quad + \sum_j \Theta(t-t_j)f_a^j(t)\,. \end{aligned} \tag{6}$$

The first term on the right-hand side of Eq. (6) is made up of a series of impulses, associated with the pumping of the atoms at times t_j into the upper lasing level. The expectation value of this term is given by

$$\left\langle \sum_j \delta(t-t_j)\sigma_a^j(t_j)\right\rangle$$

$$= \left\langle \sum_j \delta(t-t_j)\langle\sigma_a^j(t_j)\rangle\right\rangle_S = \left\langle \sum_j \delta(t-t_j)\right\rangle_S . \tag{7}$$

In the above expression, a double average is made, as mentioned before. For the quantum-mechanical average, we use the fact that the atoms are initially prepared in the upper state, so that $\langle\sigma_a^j(t_j)\rangle = 1$. The remaining classical average over the injection times is indicated by the index S on the angle brackets in Eq. (7). The average of the last sum in Eq. (7) yields the mean pumping rate R of the upper lasing level:

$$\left\langle \sum_j \delta(t-t_j)\right\rangle_S = R\int_{-\infty}^{+\infty} dt_j\delta(t-t_j) = R\,. \tag{8}$$

The same procedure is adopted for the other macroscopic atomic operators. In order to separate the drift terms from the noise terms in Eq. (6) we add and subtract the expectation value of the first term, adding the difference between the injection impulses and the rate R to the fluctuation force, which becomes then

$$F_a(t) = \sum_j \Theta(t-t_j)f_a^j(t) + \sum_j \delta(t-t_j)\sigma_a^j(t_j) - R\,. \tag{9}$$

The new Langevin operator $F_a(t)$ is the total noise operator for the macroscopic atomic population $N_a(t)$. It incorporates the fluctuations of the population of the upper level due to both radiative decay and pumping. Applying the same method to all macroscopic atomic operators, we are led to the following set of equations:

$$\dot{a}(t) = gM(t) - \frac{\gamma}{2}a(t) + \frac{\gamma}{2}\lambda + F_\gamma(t), \tag{10a}$$

$$\dot{M}(t) = g\Big[N_a(t) - N_b(t)\Big]a(t) - \Gamma M(t) + F_M(t), \tag{10b}$$

$$\begin{aligned}\dot{N}_a(t) &= R - g\Big[a^\dagger(t)M(t) + M^\dagger(t)a(t)\Big] \\ &\quad -(\Gamma_a+\Gamma'_a)N_a(t) + F_a(t),\end{aligned} \tag{10c}$$

$$\begin{aligned}\dot{N}_b(t) &= g\Big[a^\dagger(t)M(t) + M^\dagger(t)a(t)\Big] \\ &\quad -\Gamma_b N_b(t) + \Gamma'_a N_a(t) + F_b(t).\end{aligned} \tag{10d}$$

The evaluation of the correlation functions of the above Langevin forces involves the calculation of

$$I(t,t') = \left\langle \sum_{j,k} \delta(t-t_j)\delta(t'-t_k)\right\rangle_S . \tag{11}$$

This can be easily done in two extreme cases. For regular pumping, we may set $t_j = t_0 + j\tau$, where τ is the constant time interval between two successive atoms and t_0 is an arbitrary time origin. Since there are then no pump fluctuations, the average of the product of δ functions in (11) can be disentangled into the product of two separate averages, each of which is equal to the pumping rate R. We get therefore

$$\left\langle \sum_{j,k} \delta(t-t_j)\delta(t'-t_k)\right\rangle_S = R^2 \qquad \text{(regular)}. \tag{12}$$

On the other hand, for Poissonian pumping, t_j is completely uncorrelated to t_k, unless of course $j=k$. We have then

$$\left\langle \sum_{j,k} \delta(t-t_j)\delta(t'-t_k)\right\rangle_S = \left\langle \sum_j \delta(t-t_j)\delta(t'-t_j)\right\rangle_S + \left\langle \sum_{j\neq k} \delta(t-t_j)\delta(t'-t_k)\right\rangle_S = R\delta(t-t') + R^2\,. \tag{13}$$

In the general case, one gets [2]

$$\left\langle \sum_{j,k} \delta(t-t_j)\delta(t'-t_k) \right\rangle_S - R^2 = R(1-p)\delta(t-t'), \tag{14}$$

where p is a parameter that characterizes the pumping statistics: a Poissonian excitation corresponds to $p=0$, while regular pumping corresponds to $p=1$. The intermediate cases between these two extremes are described by values of p between one and zero.

Using the above results, we find that the only nonvanishing correlation forces of the Langevin forces in (10) are

$$\langle F_M^\dagger(t)F_M(t')\rangle = \left[(2\Gamma-\Gamma_a-\Gamma_a')\langle N_a(t)\rangle + R\right]\delta(t-t'), \tag{15a}$$

$$\langle F_M(t)F_M^\dagger(t')\rangle = \left[(2\Gamma-\Gamma_b)\langle N_b(t)\rangle + \Gamma_a'\langle N_a(t)\rangle\right]\delta(t-t'), \tag{15b}$$

$$\langle F_M(t)F_a(t')\rangle = (\Gamma_a+\Gamma_a')\langle M(t)\rangle\,\delta(t-t'), \tag{15c}$$

$$\langle F_M(t)F_b(t')\rangle = -\Gamma_a'\langle M(t)\rangle\,\delta(t-t'), \tag{15d}$$

$$\langle F_b(t)F_M(t')\rangle = \Gamma_b\langle M(t)\rangle\,\delta(t-t'), \tag{15e}$$

$$\langle F_a(t)F_a(t')\rangle = \left[(\Gamma_a+\Gamma_a')\langle N_a(t)\rangle + R(1-p)\right]\delta(t-t'), \tag{15f}$$

$$\langle F_a(t)F_b(t')\rangle = -\Gamma_a'\langle N_a(t)\rangle\,\delta(t-t'), \tag{15g}$$

$$\langle F_b(t)F_b(t')\rangle = \left[\Gamma_b\langle N_b(t)\rangle + \Gamma_a'\langle N_a(t)\rangle\right]\delta(t-t'). \tag{15h}$$

Equations (3), (10), and (15) describe completely the laser dynamics as well as the dynamics of the quantum fluctuations for arbitrary pumping statistics. Note that the field Langevin force already takes into account the Poisson statistics of the injected signal. That is, for all purposes an injected field in a coherent state can be considered as classical [11].

III. FLUCTUATIONS AROUND STEADY STATE

A. Normal ordering representation

The nonlinear equations for macroscopic operators obtained in the preceding section may be transformed into a more manageable form by introducing a c-number representation for the atomic and field operators. We impose the condition that the corresponding c-number equations must lead to the same results as the original operator equations for the average values of operators and second-order correlation functions. The actual form of the c-number equations will depend on the choice of the ordering for products of the atomic and field operators. We choose the normal ordering $a^\dagger, M^\dagger, N_a, N_b, M$, and a. Since Eqs. (10) are already written in normal order, the corresponding c-number equations are, simply,

$$\dot{\mathcal{A}}(t) = g\mathcal{M}(t) - \frac{\gamma}{2}\mathcal{A}(t) + \frac{\gamma}{2}\lambda + \mathcal{F}_\gamma(t), \tag{16a}$$

$$\dot{\mathcal{M}}(t) = g\left[\mathcal{N}_a(t)-\mathcal{N}_b(t)\right]\mathcal{A}(t) - \Gamma\mathcal{M}(t) + \mathcal{F}_{\mathcal{M}}(t), \tag{16b}$$

$$\dot{\mathcal{N}}_a(t) = R - g\left[\mathcal{A}^*(t)\mathcal{M}(t) + \mathcal{M}^*(t)\mathcal{A}(t)\right] - (\Gamma_a+\Gamma_a')\mathcal{N}_a(t) + \mathcal{F}_a(t), \tag{16c}$$

$$\dot{\mathcal{N}}_b(t) = g\left[\mathcal{A}^*(t)\mathcal{M}(t) + \mathcal{M}^*(t)\mathcal{A}(t)\right] - \Gamma_b\mathcal{N}_b(t) + \Gamma_a'\mathcal{N}_a(t) + \mathcal{F}_b(t), \tag{16d}$$

where the $\mathcal{F}_k(t)$ are stochastic Langevin functions with the properties

$$\langle \mathcal{F}_k(t)\rangle = 0, \tag{17a}$$

$$\langle \mathcal{F}_k(t)\mathcal{F}_l(t')\rangle = 2\mathcal{D}_{kl}\,\delta(t-t'). \tag{17b}$$

The diffusion coefficients $\mathcal{D}_{kl}$ are determined from the requirement that the c-number equations for the second momenta should be identical to the corresponding normally ordered operator equations [2]. We get then

$$2\mathcal{D}_{\mathcal{M}^*\mathcal{M}} = (2\Gamma-\Gamma_a-\Gamma_a')\langle\mathcal{N}_a(t)\rangle + R, \tag{18a}$$

$$2\mathcal{D}_{\mathcal{M}\mathcal{M}} = 2g\langle\mathcal{M}(t)\mathcal{A}(t)\rangle, \tag{18b}$$

$$2\mathcal{D}_{b\mathcal{M}} = \Gamma_b\langle\mathcal{M}(t)\rangle, \tag{18c}$$

$$2\mathcal{D}_{aa} = (\Gamma_a+\Gamma_a')\langle\mathcal{N}_a(t)\rangle + R(1-p) - g\left[\langle\mathcal{A}^*(t)\mathcal{M}(t) + \mathcal{M}^*(t)\mathcal{A}(t)\rangle\right], \tag{18d}$$

$$2\mathcal{D}_{bb} = \Gamma_b\langle\mathcal{N}_b(t)\rangle + \Gamma_a'\langle\mathcal{N}_a(t)\rangle - g\left[\langle\mathcal{A}^*(t)\mathcal{M}(t) + \mathcal{M}^*(t)\mathcal{A}(t)\rangle\right], \tag{18e}$$

$$2\mathcal{D}_{ab} = -\Gamma_a'\langle\mathcal{N}_a(t)\rangle + g\left[\langle\mathcal{A}^*(t)\mathcal{M}(t) + \mathcal{M}^*(t)\mathcal{A}(t)\rangle\right]. \tag{18f}$$

B. Steady state

The steady state is obtained from Eqs. (16) by neglecting the fluctuations and setting the time derivatives equal to zero, leading to the following set of nonlinear algebraic equations:

$$g\mathcal{M}_s - \frac{\gamma}{2}\mathcal{A}_s + \frac{\gamma}{2}\lambda = 0, \tag{19a}$$

$$R - (\Gamma_a+\Gamma_a')\mathcal{N}_{a_s} - g\left(\mathcal{A}_s^*\mathcal{M}_s + \mathcal{M}_s^*\mathcal{A}_s\right) = 0, \tag{19b}$$

$$\Gamma_a'\mathcal{N}_{a_s} - \Gamma_b\mathcal{N}_{b_s} + g\left(\mathcal{A}_s^*\mathcal{M}_s + \mathcal{M}_s^*\mathcal{A}_s\right) = 0, \tag{19c}$$

$$g(\mathcal{N}_{a_s}-\mathcal{N}_{b_s})\mathcal{A}_s - \Gamma\mathcal{M}_s = 0. \tag{19d}$$

Expressing the atomic variables in terms of the steady-state field $\mathcal{A}_s$, we get

$$\mathcal{N}_{a_s} = \frac{R}{(\Gamma_a+\Gamma_b)} + \frac{\gamma\Gamma\Gamma_b}{2g^2(\Gamma_a+\Gamma_b)}\left(1-\frac{\lambda}{\mathcal{A}_s}\right), \tag{20a}$$

$$\mathcal{N}_{a_s} - \mathcal{N}_{b_s} = \frac{\gamma\Gamma}{2g^2}\left(1-\frac{\lambda}{\mathcal{A}_s}\right), \tag{20b}$$

$$\mathcal{M}_s = \frac{\gamma}{2g}\left(1-\frac{\lambda}{\mathcal{A}_s}\right)\mathcal{A}_s, \tag{20c}$$

where $\mathcal{A}_s$ is a solution of the equation

$$\frac{g^2R(\Gamma_b-\Gamma'_a)}{(\Gamma_a+\Gamma'_a)\Gamma_b\Gamma+2g^2(\Gamma_a+\Gamma_b)|\mathcal{A}_s|^2}\mathcal{A}_s-\frac{\gamma}{2}\mathcal{A}_s+\frac{\gamma}{2}\lambda=0. \tag{21}$$

The above equation may be written in terms of the normalized intensities for the laser with (I) and without (I_0) an injected signal,

$$I=\frac{|\mathcal{A}_s|^2}{|\mathcal{A}_{\rm sat}|^2},\quad I_0=\frac{|\mathcal{A}_0|^2}{|\mathcal{A}_{\rm sat}|^2},$$

respectively, where

$$|\mathcal{A}_{\rm sat}|^2=\frac{\Gamma_a+\Gamma'_a}{\Gamma_a+\Gamma_b}\frac{\Gamma\Gamma_b}{2g^2} \tag{22}$$

is the saturation intensity for $\lambda=0$ and

$$|\mathcal{A}_0|^2=|\mathcal{A}_{\rm sat}|^2\left(\frac{R}{R_T}-1\right) \tag{23}$$

is the steady-state intensity for above-threshold operation ($R>R_T$) without an injected field ($\lambda=0$), expressed in terms of the threshold atomic pumping rate

$$R_T=\frac{\gamma\Gamma\Gamma_b}{2g^2}\frac{(\Gamma_a+\Gamma'_a)}{(\Gamma_b-\Gamma'_a)}. \tag{24}$$

Equation (21) becomes then

$$\lambda=\frac{I-I_0}{I+1}\mathcal{A}_s. \tag{25}$$

It is clear, from Eq. (25), that the ratio $\lambda/\mathcal{A}_s$ is real and lies between -1 and $+1$. Therefore, the steady-state value of the cavity-field phase is $\phi_s=\beta+n\pi$, where $n=0, 1, \ldots$, and β is the injected-signal phase ($\lambda=|\lambda|e^{i\beta}$).

The normalized injected-signal intensity $I_\lambda=|\lambda|^2/|\mathcal{A}_{\rm sat}|^2$ is related to the normalized cavity-field intensity through the expression

$$I_\lambda=\frac{(I-I_0)^2}{(I+1)^2}I, \tag{26}$$

obtained by squaring Eq. (25).

Equations (25) and (26) are plotted in Fig. 1. From curve (a), one can see that there are three possible branches for laser operation above threshold. The two lowest ones correspond to a cavity-field phase differing by an odd number of π's from the injected signal phase. In the Appendix we show that these two branches are always unstable. The stability of the upper branch is also checked in the Appendix.

C. Quantum fluctuations

We investigate now the small fluctuations of the field and atomic variables around the steady state, assuming, as usual, each of these variables as being a sum of its steady-state value and a small fluctuating term:

$$\begin{aligned}\mathcal{A}(t)&=\mathcal{A}_s+\delta\mathcal{A}(t),\\ \mathcal{M}(t)&=\mathcal{M}_s+\delta\mathcal{M}(t),\\ \mathcal{N}_a(t)&=\mathcal{N}_{a_s}+\delta\mathcal{N}_a(t),\\ \mathcal{N}_b(t)&=\mathcal{N}_{b_s}+\delta\mathcal{N}_b(t).\end{aligned}$$

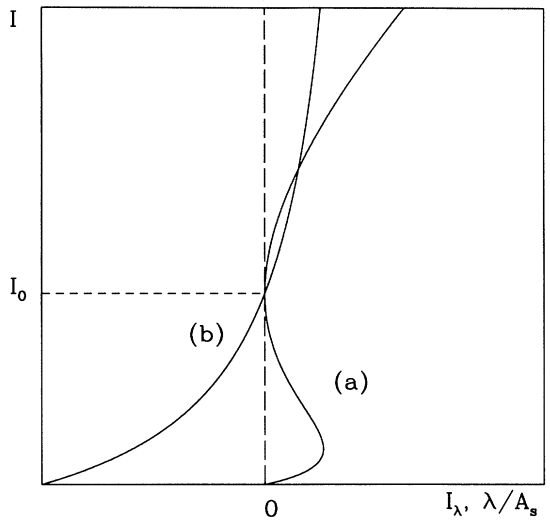

FIG. 1. Normalized steady-state intensity I versus (a) normalized injected-signal intensity I_λ, Eq. (26), and (b) ratio between injected-signal and cavity-field amplitudes $\lambda/\mathcal{A}_s$, Eq. (25), for above-threshold laser operation.

Substituting these expressions into Eqs. (16) and neglecting higher-order terms in the fluctuations, we arrive at the following set of linear differential equations:

$$\delta\dot{\mathcal{A}}(t)=-\frac{\gamma}{2}\delta\mathcal{A}(t)+g\delta\mathcal{M}(t)+\mathcal{F}_\gamma(t), \tag{27a}$$

$$\delta\dot{\mathcal{M}}(t)=-\Gamma\delta\mathcal{M}(t)+g(\mathcal{N}_{a_s}-\mathcal{N}_{b_s})\delta\mathcal{A}(t)+g[\delta\mathcal{N}_a(t)-\delta\mathcal{N}_b(t)]\mathcal{A}_s+\mathcal{F}_\mathcal{M}(t), \tag{27b}$$

$$\delta\dot{\mathcal{N}}_a(t)=-(\Gamma_a+\Gamma'_a)\delta\mathcal{N}_a(t)-g[\mathcal{A}_s^*\delta\mathcal{M}(t)+\mathcal{A}_s\delta\mathcal{M}^*(t)]-g[\mathcal{M}_s\delta\mathcal{A}^*(t)+\mathcal{M}_s^*\delta\mathcal{A}(t)]+\mathcal{F}_a(t), \tag{27c}$$

$$\delta\dot{\mathcal{N}}_b(t)=-\Gamma_b\delta\mathcal{N}_b(t)+\Gamma'_a\delta\mathcal{N}_a(t)+g[\mathcal{A}_s^*\delta\mathcal{M}(t)+\mathcal{A}_s\delta\mathcal{M}^*(t)]+g[\mathcal{M}_s\delta\mathcal{A}^*(t)+\mathcal{M}_s^*\delta\mathcal{A}(t)]+\mathcal{F}_b(t). \tag{27d}$$

These equations are now converted into algebraic equations by introducing the Fourier transforms of the field and atomic variables (for simplicity, we use the same notation for both functions of the Fourier transform pair, differentiating them therefore through their arguments):

$$\begin{aligned}\delta G(t)&=\frac{1}{\sqrt{2\pi}}\int_{-\infty}^{\infty}\delta G(\omega)e^{-i\omega t}\,d\omega,\\ \delta G(\omega)&=\frac{1}{\sqrt{2\pi}}\int_{-\infty}^{\infty}\delta G(t)e^{i\omega t}\,dt,\end{aligned} \tag{28}$$

so that

$$-i\omega\delta\mathcal{A}(\omega) = -\frac{\gamma}{2}\delta\mathcal{A}(\omega) + g\delta\mathcal{M}(\omega), \tag{29a}$$

$$-i\omega\delta\mathcal{M}(\omega) = -\Gamma\delta\mathcal{M}(\omega) + g(\mathcal{N}_{a_s} - \mathcal{N}_{b_s})\delta\mathcal{A}(\omega) + g[\delta\mathcal{N}_a(\omega) - \delta\mathcal{N}_b(\omega)]\mathcal{A}_s + \mathcal{F}_{\mathcal{M}}(\omega), \tag{29b}$$

$$\begin{aligned}-i\omega\delta\mathcal{N}_a(\omega) &= -(\Gamma_a + \Gamma'_a)\delta\mathcal{N}_a(\omega) \\ &\quad -g\left[\mathcal{A}_s^*\delta\mathcal{M}(\omega) + \mathcal{A}_s\delta\mathcal{M}^*(-\omega)\right] \\ &\quad -g\left[\mathcal{M}_s\delta\mathcal{A}^*(-\omega) + \mathcal{M}_s^*\delta\mathcal{A}(\omega)\right] + \mathcal{F}_a(\omega), \\ -i\omega\delta\mathcal{N}_b(\omega) &= -\Gamma_b\delta\mathcal{N}_b(\omega) + \Gamma'_a\delta\mathcal{N}_a(\omega) \\ &\quad +g\left[\mathcal{A}_s^*\delta\mathcal{M}(\omega) + \mathcal{A}_s\delta\mathcal{M}^*(-\omega)\right] \\ &\quad +g\left[\mathcal{M}_s\delta\mathcal{A}^*(-\omega) + \mathcal{M}_s^*\delta\mathcal{A}(\omega)\right] + \mathcal{F}_b(\omega).\end{aligned} \tag{29c}$$

In the above equations, we have set $\mathcal{F}_\gamma(t) = 0$, since its mean value and all normal-ordered correlation functions are equal to zero at zero temperature, in view of (3). This is actually one of the advantages of using normal ordering: (3b) implies that this will not be true for other orderings.

It is straightforward to solve Eqs. (29). As we are interested on the spectra of fluctuations of the field quadrature components, we write the Fourier amplitudes of the field fluctuations $\delta\mathcal{A}(\omega)$ and $\delta\mathcal{A}^*(-\omega)$ in terms of the Fourier transform of the Langevin functions. We get finally

$$\begin{aligned}\delta\mathcal{A}(\omega) = \frac{ig}{D(\omega)}\Bigg\{C(\omega)\Bigg[\frac{\Gamma_b - \Gamma'_a - i\omega}{\Gamma_a + \Gamma'_a - i\omega}g\mathcal{A}_s\mathcal{F}_a(\omega) \\ -g\mathcal{A}_s\mathcal{F}_b(\omega)\Bigg] + \{[C(\omega) + |\mathcal{A}_s|^2]\mathcal{F}_{\mathcal{M}}(\omega) \\ -\mathcal{A}_s^2\mathcal{F}_{\mathcal{M}}^*(-\omega)\}(\Gamma_b - i\omega)\Bigg\},\end{aligned} \tag{30}$$

where

$$C(\omega) = \frac{\left[\left(\frac{\gamma\Gamma}{2}\frac{\lambda}{\mathcal{A}_s} - \omega^2\right) - i\omega\left(\Gamma + \frac{\gamma}{2}\right)\right](\Gamma_a + \Gamma'_a - i\omega)(\Gamma_b - i\omega)}{g^2(\Gamma_b + \Gamma_a - 2i\omega)\left[\frac{\gamma}{2}\left(2 - \frac{\lambda}{\mathcal{A}_s}\right) - i\omega\right]},$$

$$D(\omega) = \omega[C(\omega) + 2|\mathcal{A}_s|^2]\left[\left(\frac{\gamma}{2} + \Gamma\right) - i\omega - \frac{\Gamma\gamma}{2i\omega}\frac{\lambda}{\mathcal{A}_s}\right](\Gamma_b - i\omega).$$

The expression for $\delta\mathcal{A}^*(-\omega)$ is obtained by performing the complex conjugation and substituting ω by $-\omega$ in Eq. (30).

We choose the injected signal as real, which leads to a real steady-state field. In this case, the amplitude and phase quadrature components of the cavity-field fluctuations are defined, respectively, as

$$\delta X(\omega) = \frac{1}{2}[\delta\mathcal{A}(\omega) + \delta\mathcal{A}^*(-\omega)], \tag{31a}$$

$$\delta Y(\omega) = \frac{1}{2i}[\delta\mathcal{A}(\omega) - \delta\mathcal{A}^*(-\omega)]. \tag{31b}$$

Note that $\delta X^*(\omega) = \delta X(-\omega)$ and $\delta Y^*(\omega) = \delta Y(-\omega)$, so that $\delta X(t)$ and $\delta Y(t)$ are real, as expected.

Replacing Eq. (30) for $\delta\mathcal{A}(\omega)$ — as well as the corresponding expression for $\delta\mathcal{A}^*(-\omega)$ — in (31), we arrive at the following expressions for the quadrature components:

$$\begin{aligned}\delta X(\omega) = &\frac{(\Gamma_a + \Gamma'_a - i\omega)}{g(\Gamma_a + \Gamma_b - 2i\omega)\left(\gamma - \frac{\gamma}{2}\frac{\lambda}{\mathcal{A}_s} - i\omega\right)[C(\omega) + 2|\mathcal{A}_s|^2]} \\ &\times\left[(\Gamma_b - i\omega)\frac{\mathcal{F}_{\mathcal{M}}(\omega) + \mathcal{F}_{\mathcal{M}}^*(-\omega)}{2} + g\mathcal{A}_s\frac{\Gamma_b - \Gamma'_a - i\omega}{\Gamma_a + \Gamma'_a - i\omega}\mathcal{F}_a(\omega) - g\mathcal{A}_s\mathcal{F}_b(\omega)\right],\end{aligned} \tag{32a}$$

$$\delta Y(\omega) = \frac{-ig}{2\left[\left(\frac{\gamma\Gamma}{2}\frac{\lambda}{\mathcal{A}_s} - \omega^2\right) - i\omega\left(\frac{\gamma}{2} + \Gamma\right)\right]}\left[\mathcal{F}_{\mathcal{M}}(\omega) - \mathcal{F}_{\mathcal{M}}^*(-\omega)\right]. \tag{32b}$$

It is easy to see that the Fourier-transformed Langevin noise functions obey the equations

$$\langle\mathcal{F}_k(\omega)\mathcal{F}_l(\omega')\rangle = 2\mathcal{D}_{kl}\,\delta(\omega + \omega'),$$

which result from the fact that the correlation functions of the time-dependent fluctuation forces depend only on the time differences (stationary process). In view of this, the autocorrelation and cross-correlation functions of the amplitude and phase quadrature components are δ correlated:

$$\langle\delta X(\omega)\delta X(\omega')\rangle = (\delta X^2)_\omega\,\delta(\omega + \omega'), \tag{33a}$$

$$\langle\delta Y(\omega)\delta Y(\omega')\rangle = (\delta Y^2)_\omega\,\delta(\omega + \omega'), \tag{33b}$$

$$\langle\delta X(\omega)\delta Y(\omega')\rangle = (\delta X\delta Y)_\omega\,\delta(\omega + \omega'). \tag{33c}$$

We calculate now the power spectra of the amplitude and phase quadrature components of the cavity-field fluctuations, defined as the Fourier transform,

$$\mathcal{W}_X(\omega) = \int_{-\infty}^{\infty} e^{i\omega t}\langle \delta X(0)\delta X(t)\rangle\, dt,$$

with an analogous definition for $\mathcal{W}_Y(\omega)$. Upon replacing $\delta X(0)$ and $\delta X(t)$ in this expression by their Fourier transforms (28), it is easy to show that $\mathcal{W}_X(\omega) = (\delta X^2)_\omega$, where $(\delta X^2)_\omega$ is defined by Eq. (33a).

From Eqs. (18), (32), and (33), we get the following expressions for the spectra of the quadrature components of the cavity-field fluctuations:

$$(\delta X^2)_\omega = \frac{(\Gamma_a+\Gamma_a')^2+\omega^2}{g^2\left[(\Gamma_a+\Gamma_b)^2+4\omega^2\right]\left[\frac{\gamma^2}{4}\left(2-\frac{\lambda}{\mathcal{A}_s}\right)^2+\omega^2\right]\left|C(\omega)+2\mathcal{A}_s^2\right|^2}$$
$$\times\left\{\Gamma\Gamma_b^2\mathcal{N}_{a_s}+\omega^2\left[R+(\Gamma-\Gamma_a-\Gamma_a')\mathcal{N}_{a_s}\right]+\frac{2g^2\mathcal{A}_s^2\mathcal{N}_{a_s}}{(\Gamma_a+\Gamma_a')^2+\omega^2}\left[\Gamma_b(\Gamma_a+\Gamma_a')(\Gamma_a+\Gamma_b)+2\omega^2(\Gamma_a+2\Gamma_a')\right]\right.$$
$$\left.-\frac{g^2\mathcal{A}_s^2R}{(\Gamma_a+\Gamma_a')^2+\omega^2}\left[(\Gamma_b-\Gamma_a')\left(p\Gamma_b+2\Gamma_a+(2-p)\Gamma_a'\right)+\omega^2(p+2)\right]\right\}, \tag{34a}$$

$$(\delta Y^2)_\omega = \frac{g^2\Gamma\mathcal{N}_{a_s}}{\left[\left(\frac{\gamma\Gamma}{2}\frac{\lambda}{\mathcal{A}_s}-\omega^2\right)^2+\omega^2\left(\frac{\gamma}{2}+\Gamma\right)^2\right]}, \tag{34b}$$

and $(\delta X\delta Y)_\omega = 0$.

IV. FLUCTUATIONS SPECTRA OF THE OUTPUT FIELD

We investigate now the fluctuations spectra of the field transmitted through the cavity port. We use well-known methods [12,13] which allow us to calculate these spectra from the correlation functions of the internal field, given by Eqs. (33) and (34). The normalized spectrum of fluctuations corresponding to a quadrature

$$X_\theta = a_{\rm out}(t)e^{-i\theta} + a_{\rm out}^\dagger(t)e^{i\theta} \tag{35}$$

is defined as

$$V(\theta,\omega) = \int_{-\infty}^{\infty} e^{i\omega\tau}\langle X_\theta(t+\tau), X_\theta(t)\rangle\, d\tau, \tag{36}$$

where $\langle X,Y\rangle = \langle XY\rangle - \langle X\rangle\langle Y\rangle$. For a stationary field this quantity is time independent.

Expression (36) can be related to the c-number averages of the field fluctuations defined in the normally ordered representation [12,13]. Hence the spectrum of output fluctuations for a quadrature component, defined by the angle θ, can be written in terms of the correlation functions for the quadrature components $\delta X(\omega)$ and $\delta Y(\omega)$ of the intracavity field fluctuations (neglecting internal losses):

$$V(\theta,\omega) = 1+4\gamma\left[(\delta X^2)_\omega\cos^2\theta + (\delta Y^2)_\omega\sin^2\theta + 2(\delta X\delta Y)_\omega\cos\theta\sin\theta\right]. \tag{37}$$

The first term on the right-hand side of the above equation comes from the commutator of the outgoing boson operators and corresponds to the shot-noise contribution. For a coherent state, $V(\theta,\omega)=1$. Therefore, $V(\theta,\omega)<1$ means that we have found squeezing in a quadrature component defined by θ. Complete squeezing at some frequency ω occurs when $V(\theta,\omega)=0$.

The spectrum of amplitude fluctuations is obtained from the above equation by setting $\theta=0$, while for $\theta=\pi/2$ one gets the spectrum of phase fluctuations. For θ between those two angles, Eq. (37) produces the spectrum of fluctuations in a quadrature component, which is a mixture of amplitude and phase quadrature components. It is straightforward to show that the best squeezing occurs when

$$\cos 2\theta = -\frac{\mathrm{Re}\,S(\omega)}{|S(\omega)|}, \qquad \sin 2\theta = -\frac{\mathrm{Im}\,S(\omega)}{|S(\omega)|},$$

where $S(\omega) = (\delta X^2)_\omega - (\delta Y^2)_\omega + 2i(\delta X\delta Y)_\omega$. Since $(\delta X\delta Y)_\omega$ is zero, due to a perfect resonance between cavity, atoms, and injected signal, the best squeezing is, in this case, obtained for $\theta=0$ (amplitude quadrature), when $V(\omega)$ becomes

$$V_A(\omega) = 1+4\gamma(\delta X^2)_\omega\,. \tag{38}$$

We turn our attention therefore to the amplitude fluctuations spectrum.

In order to simplify the analysis, we define the dimensionless variables

$$x\equiv\lambda/\mathcal{A}_s \quad \tilde\omega\equiv\omega/\gamma, \quad a\equiv\Gamma_a/\gamma,$$
$$b\equiv\Gamma_b/\gamma, \quad c\equiv\Gamma/\gamma, \quad a'\equiv\Gamma_a'/\gamma. \tag{39}$$

In terms of these new variables, Eq. (20a) can be rewritten as

$$\mathcal{N}_{a_s} = \frac{1}{\gamma(a+b)}\left[R+R_T\frac{(b-a')}{(a+a')}(1-x)\right], \tag{40}$$

while, from (34a) and (40), Eq. (38) becomes

$$V_A(\tilde{\omega}) = 1 + \frac{2bc(a+a')}{(b-a')}\frac{1}{D(\tilde{\omega})}\left\{(b^2+\tilde{\omega}^2)[(a+a')^2+\tilde{\omega}^2]\left[r+\left(\frac{c}{a+a'}-1\right)n\right]\right.$$
$$+2w^2\left[[(b-a')^2+\tilde{\omega}^2]\left(n-\tfrac{1}{2}pr\right)-[(b-a')(a+a')+\tilde{\omega}^2]\left[r-\frac{a+2a'}{a+a'}n\right]\right.$$
$$\left.\left.+[(a+a')^2+\tilde{\omega}^2]\left(\frac{a'}{a+a'}n-\frac{b}{c}\frac{(b-a')}{(a+a')}(1-x)\right)\right]\right\}, \tag{41}$$

where $r \equiv R/R_T$ is the dimensionless pumping parameter. We also used the definitions

$$n = \frac{1}{(a+b)}\left[r(a+a')+(b-a')(1-x)\right], \quad w^2 = \frac{bc(a+a')}{2(a+b)}I,$$

$$D(\tilde{\omega}) = \left|\left[\tfrac{1}{2}cx-\tilde{\omega}^2-i\tilde{\omega}\left(c+\tfrac{1}{2}\right)\right](a+a'-i\tilde{\omega})(b-i\tilde{\omega})\right.$$
$$\left.+2w^2(b+a-2i\tilde{\omega})\left[\tfrac{1}{2}(2-x)-i\tilde{\omega}\right]\right|^2.$$

It is worth noticing that so far we have not made any assumptions about the relative magnitudes of the atomic and cavity decay rates. The expression for the amplitude fluctuations spectrum, Eq. (41), is completely general. However, that expression is quite long and does not allow a deeper analysis unless we take some special choices of parameters. In order to make this choice as systematically as possible we use the classification, introduced by Abraham *et al.* [14], for single-mode lasers, in terms of relations between the magnitudes of the cavity and atomic decay rates. According to this classification, single-mode lasers can be grouped into four main classes, namely, (i) $\Gamma, \Gamma_a, \Gamma_b, \Gamma'_a \gg \gamma$, dye lasers; (ii) $\Gamma \gg \gamma \sim \Gamma_a, \Gamma_b, \Gamma'_a$, helium-neon (0.6 and 1.15 μm) and argon-ion lasers; (iii) $\Gamma \gg \gamma \gg \Gamma_a, \Gamma_b, \Gamma'_a$, ruby, Nd:YAG (yttrium aluminum garnet), carbon dioxide, and semiconductor lasers; and (iv) $\gamma \gg \Gamma, \Gamma_a, \Gamma_b, \Gamma'_a$, near-infrared noble-gas lasers and many far-infrared gas lasers (including He-Ne at 3.39 μm). We start our analysis of the spectrum of amplitude fluctuations with the first of the above classes of lasers.

A. First class of lasers

This is the simplest case, where the atomic decay is much faster than the field relaxation. Usually, when considering just this case, one proceeds to the adiabatic elimination of the atomic variables. It corresponds, in our case, to the limit $a, b, c, a' \gg 1$. Under these conditions, we calculate in the following both the spectrum of amplitude fluctuations and the photon-number variance.

1. Amplitude fluctuations

In the limit $a, b, c, a' \gg 1$ and for dimensionless frequencies of the order of unity $\tilde{\omega} \sim 1$, Eq. (41) reduces to

$$V_A(\tilde{\omega}) = 1 - \frac{4r(1-x)^2}{4r^2\tilde{\omega}^2+\left[r(x-2)+2(x-1)^2\right]^2}$$
$$\times\left[\frac{b-a'}{a+b}p\left(\frac{r}{1-x}-1\right)-2\frac{(a+a')}{(a+b)}\frac{a'}{(b-a')}\right.$$
$$\left.\times\left(\frac{r}{1-x}-1\right)-\frac{2b}{b-a'}\right]. \tag{42}$$

The above expression can be simplified even more if we set $r \gg 1$, i.e., consider the laser operating far above threshold. In particular, assuming regular pumping ($p = 1$) and setting $a' = 0$, we get

$$V_A(\tilde{\omega}) = 1 - \frac{1-x}{\tilde{\omega}^2+\frac{1}{4}(x-2)^2}\frac{b}{(a+b)}. \tag{43}$$

Expression (43) is fully discussed in Ref. [6] for zero injected signal ($x = 0$). It reproduces, in that case, the known result [1] that complete squeezing at zero frequency is achieved for a decay rate of the lower atomic level much higher than the decay rate of the upper one ($b \gg a$).

The presence of an injected signal modifies the previous result in two ways. We see from (43) that, for operation far above threshold, the injected signal reduces the amount of squeezing at $\omega = 0$, which becomes vanishingly small as x approaches its upper limit 1. On the other hand, the injected signal produces an enhancement of noise reduction for laser operation not far above threshold. This effect is clearly displayed in Fig. 2, where we compare, for three different values of the pumping rate, normalized spectra of amplitude fluctuations with and without the injected signal, the amplitude of the injected signal being chosen so as to maximize squeezing, for a given pumping rate. Notice that the closer to the threshold, the higher the discrepancy between the results for lasers with and without an injected signal. From this analysis, the advantage of injecting a signal in order to increase squeezing becomes evident.

Squeezing at low pumping rates with the injection of an external signal in lasers of the first class was studied by Agarwal *et al.* [15] in the case that the signal is injected from the side, i.e., driving the atoms directly, and within the framework of a perturbative treatment of the laser field. It is easy to show [16] that these two models, driving the cavity or driving the active atoms, can be transformed one into the other, the only difference being a displacement of the cavity-field amplitude. Our analysis, being nonperturbative, extends, however, the

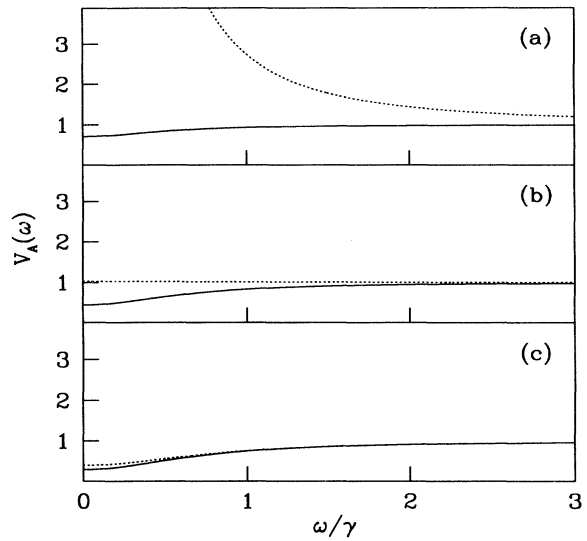

FIG. 2. Normalized spectra of amplitude fluctuations for the first class of lasers. Dotted and solid curves correspond to lasers without and with an injected signal, respectively. Curves corresponding to different pumping rates are plotted. (a) $r = 1.1$ and $x = 0.83$; (b) $r = 3$ and $x = 0.58$; (c) $r = 5$ and $x = 0.4$. For all curves $a' = 0$, $a = 10$, $b = 5 \times 10^2$, and $p = 1$. The values of the variable x for the solid curves were chosen in order to produce the best noise reduction for each value of r, by minimization of expression (42).

previous results over the whole range of laser intensities, including the region far above threshold, where the possibility of getting important squeezing was pointed out before [1,2,6].

2. *Photon-number variance*

In previous treatments [1,2,6], special attention has been given to the photon-number variance of the intracavity field. This quantity can be easily expressed in terms of the spectrum of amplitude fluctuations of the output field, starting from the relation

$$\langle(\Delta N^2\rangle = \langle N\rangle + \langle(\Delta\rho)^2\rangle\,, \tag{44}$$

where $\langle(\Delta\rho)^2\rangle$ is the normal-ordered steady-state variance [this contribution vanishes for a coherent state, so that (44) yields, in this case, the characteristic result of a Poisson distribution]. Sufficiently far above threshold, so that the field fluctuations are much smaller than the steady-state field amplitude, we may write

$$\Delta\rho(t) = \delta\mathcal{A}^2(t) \approx 2\mathcal{A}_s\delta X(t)\,, \tag{45}$$

since $\mathcal{A}_s$, the steady-state amplitude, is taken to be real and δX represents the amplitude fluctuation. This relation should be approximately valid in the case that the squeezing is not too pronounced, which is the case here (we get at most a 50% reduction in the photon-number fluctuation, far away from the minimum possible photon-number variance of a squeezed state, given approximately by $\langle N\rangle^{2/3}$; see Ref. [17]). For stronger amplitude squeezing, the photon-number distribution broadens away, becoming super-Poissonian and oscillatory, which can be explained in terms of the interference in phase space between the squeezed state and the number states [18]. Therefore,

$$\langle(\Delta\rho)^2\rangle \approx 4\mathcal{A}_s^2\langle[\delta X(t)]^2\rangle\,. \tag{46}$$

On the other hand, from (28) and (33a), we get

$$\langle[\delta X(t)]^2\rangle = \frac{1}{2\pi}\int_{-\infty}^{+\infty} d\omega(\delta X^2)_\omega\,. \tag{47}$$

From Eqs. (44), (46), and (47) and identifying $\mathcal{A}_s^2$ with $\langle n\rangle$, we get

$$\langle\Delta N^2\rangle = \langle N\rangle\left[1 + \frac{2}{\pi}\int_{-\infty}^{+\infty} d\omega(\delta X^2)_\omega\right], \tag{48}$$

which can be expressed in terms of the spectrum of amplitude fluctuations of the output field by using (38)

$$\langle\Delta N^2\rangle = \langle N\rangle\left\{1 + \frac{1}{2\pi}\int_{-\infty}^{+\infty}[V_A(\tilde\omega) - 1]\,d\tilde\omega\right\}. \tag{49}$$

For the first class of lasers the amplitude fluctuations spectrum is given by Eq. (42). Neglecting for simplicity the nonradiative decay between the two resonant atomic levels (this corresponds to setting $a' = 0$), we get then

$$\langle(\Delta N)^2\rangle = \langle N\rangle\left\{1 + \frac{(1-x)}{(a+b)} \times\left[\frac{2(a+b)(1-x) + bp(1-x-r)}{2(r-1) - x(r-4) - 2x^2}\right]\right\}, \tag{50}$$

which is a generalization of expressions previously obtained in the literature (see, for instance, [1]). Far above threshold ($r \gg 1$), the photon-number variance becomes

$$\langle\Delta N^2\rangle = \langle N\rangle\left\{1 - \frac{bp(1-x)}{(a+b)(2-x)}\right\}. \tag{51}$$

Setting also $b \gg a$ and $x = 0$, we recover the well-known result [1]

$$\langle\Delta N^2\rangle = \langle N\rangle\left(1 - \frac{p}{2}\right). \tag{52}$$

B. Second and third classes of lasers

We treat now together the second and the third classes of lasers, since both require the same approximation $c \gg 1$ in Eq. (41) for the normalized spectrum of amplitude fluctuations. Setting $c \to \infty$ in that expression and keeping the parameters a and b arbitrary, we get

$$V_A(\tilde\omega) = 1 + \frac{2ac^2}{D(\tilde\omega)}\left\{(b^2+\tilde\omega^2)(a^2+\tilde\omega^2)\frac{n}{a} + \frac{ab}{(a+b)}\left(\frac{r}{1-x} - 1\right) \times\left[(b^2+\tilde\omega^2)\left(n - \tfrac{1}{2}pr\right) - (ba+\tilde\omega^2)(r-n)\right]\right\}, \tag{53}$$

where

$$D(\tilde{\omega}) = D_1(\tilde{\omega}) + D_2(\tilde{\omega}) + D_3(\tilde{\omega}),$$

with

$$D_1(\tilde{\omega}) = c^2\left(\tfrac{1}{4}x^2 + \tilde{\omega}^2\right)(a^2 + \tilde{\omega}^2)(b^2 + \tilde{\omega}^2),$$

$$D_2(\tilde{\omega}) = \frac{a^2b^2c^2}{(a+b)^2}\left(\frac{r}{1-x} - 1\right)^2 \times\left[(a+b)^2 + 4\tilde{\omega}^2\right]\left[\tfrac{1}{4}(2-x)^2 + \tilde{\omega}^2\right],$$

$$D_3(\tilde{\omega}) = \frac{abc^2}{2(a+b)}\left(\frac{r}{1-x} - 1\right) \times\left\{(\tilde{\omega}^2 + ab)(a+b)\left[4\tilde{\omega}^2 + x(2-x)\right] - 4\tilde{\omega}^2(1-x)(2\tilde{\omega}^2 + a^2 + b^2)\right\}.$$

For simplicity, we have made $a' = 0$ in the above expressions.

As in the case where no signal is injected [6], expression (53) exhibits noise reduction even with Poissonian atomic pumping. This results from the negative contribution of the last term on the right-hand side of Eq. (53), which does not depend on p. Because this contribution is proportional to r^2 for large r, while the remaining positive terms become proportional to r, we consider the situation $r \gg 1$, corresponding to far-above-threshold laser operation. In order to keep only this negative contribution, we set $p = 0$, thus isolating it from the effects associated with the regularization of the atomic pumping. We obtain therefore

$$V_A(\tilde{\omega}) = 1 + \frac{2(1-x)(a-b)\tilde{\omega}^2}{b\left[(a+b)^2 + 4\tilde{\omega}^2\right]\left[\tfrac{1}{4}(2-x)^2 + \tilde{\omega}^2\right]}. \quad (54)$$

Setting $a \ll b$, in order to obtain maximum noise reduction, we arrive at

$$V_A(\tilde{\omega}) = 1 - \frac{2(1-x)\tilde{\omega}^2}{(b^2 + 4\tilde{\omega}^2\left(\tfrac{1}{4}(2-x)^2 + \tilde{\omega}^2\right)}, \quad (55)$$

which shows a minimum noise level

$$V_A(\tilde{\omega})_{\min} = 1 - \frac{2(1-x)}{[b+2-x]^2} \quad (56)$$

at the frequency $\tilde{\omega}_0 = \sqrt{b(2-x)/4}$. From Eq. (56) one can see that, as for the first class, squeezing is smaller in the presence of the injected signal. However, as before, lasers with an injected signal exhibit squeezing for pumping parameters much lower than lasers without that signal, as displayed in Fig. 3.

In Fig. 3(a) one observes that a strong injected signal can lead to squeezing for a pumping rate of the order of 10^2, which is not enough to achieve squeezing in lasers with no injected signal. On the other hand, Fig. 3(b) shows the increase in noise levels when a signal is injected at higher pumping rates. As in the first class of lasers, injecting a signal allows the production of squeezing closer to threshold, but spoils noise compression for very high pumping rates.

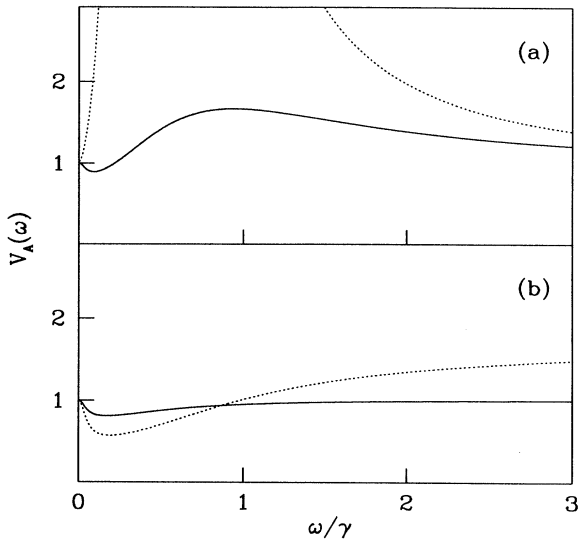

FIG. 3. Normalized spectra of amplitude fluctuations for second and third classes of lasers with pumping parameters (a) $r = 10^2$ and (b) $r = 10^4$. Dotted curves correspond to lasers without an injected signal, while the solid curves correspond to lasers with the injection of a strong signal ($x = 0.85$). For all curves $a' = 0$, $a = 10^{-3}$, $b = 10^{-1}$, $c \gg 1$, and the pumping is Poissonian ($p = 0$).

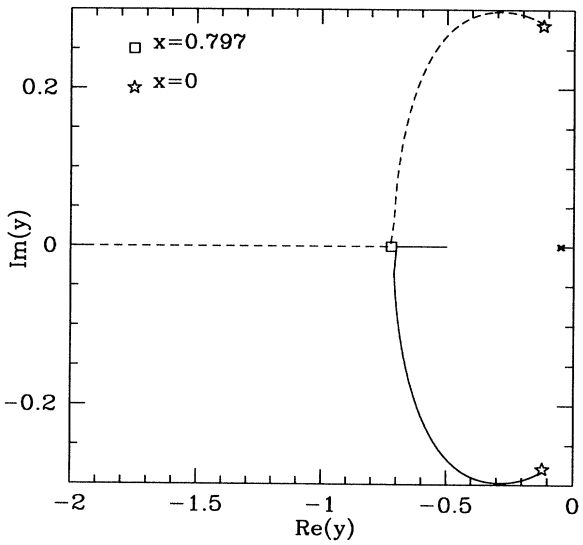

FIG. 4. Behavior of the three roots of the characteristic polynomial corresponding to the second and the third class of lasers, for a pumping rate $r = 10^2$. The three roots are represented by a dashed line, a solid line, and the symbol $\times$, respectively. The normalized injected field changes from 0 to 1. For $x = 0$, two of the roots are complex conjugates, with the real part approximately equal to -0.1 and the imaginary part approximately equal to 0.3. As x increases, the imaginary part of the two complex roots first increases and then decreases down to zero, when $x = 0.797$, while the real root remains practically unaffected. From then on these roots become real and distinct.

In fact, squeezing for a zero injected signal at $r = 10^2$ is destroyed by the "quasiunstable" behavior in this region of parameters. This is the origin of the peak present in Fig. 3(a). Indeed, the roots of the characteristic polynomial of the drift matrix, given by Eq. (A 2) of the Appendix, are displayed in Fig. 4. One finds that, for a zero injected signal, there are two complex-conjugate roots and one real root. The real part of those roots is negative, indicating stable behavior, but its absolute value is very small (that is, much smaller than 1), justifying our denomination quasiunstable. The real root would tend to increase noise at zero frequency. This effect is balanced, however, by a vanishing numerator in the expression for the spectrum [cf. Eq. (54)]. On the other hand, the imaginary parts of the two complex-conjugate roots, in absolute value, coincide with the normalized frequency $\tilde{\omega}$ where the peak occurs. For $r = 10^2$, the magnitude of those imaginary parts is $\tilde{\omega} \approx 1$, leading to the peak exhibited in Fig. 3(a). As the pumping rate is increased, the magnitude of the imaginary parts of the complex-conjugate roots is displaced towards higher values of $\tilde{\omega}$ (for $r = 10^4$ we get $\tilde{\omega} \approx 8$), so the noise peak is displaced outside the region of interest. This explains the absence of a peak in Fig. 3(b). As the intensity of the injected signal is increased, the real part of the two complex roots becomes more negative (see Fig. 4). When a strong signal ($x > 0.797$) is injected, the two complex roots become real, with large negative values. This allows squeezing to be seen, as shown in Fig. 3(a).

C. Fourth class of lasers

This is the case where the dynamics of the atomic polarization is fully considered. We analyze this class of lasers graphically. The parameters are chosen so that the steady state is stable, according to the analysis developed in the Appendix. Figure 5 shows comparisons between normalized spectra of amplitude fluctuations for lasers without an injected signal and those with a strong signal injected, operating far above threshold, where the former displays squeezing even for Poissonian pumping, as pointed out in Ref. [6]. Again, in this limit (far above threshold), the injected signal increases the noise level, but it decreases the pumping rate needed for achieving the squeezing, as one can see from Fig. 5(a). That figure displays a situation ($r = 10^2$) where squeezing is not reached without the injected signal, but a noise level 11% below shot-noise is obtained with a strong injected signal.

For regular pumping, the situation is even better. This feature is shown in Fig. 6, where squeezing is obtained with an intense injected signal for a pumping rate as low as three times the threshold pumping rate. Here again, we notice the presence of a quasiunstable behavior, which can, as before, be analyzed in terms of the roots of the characteristic polynomial of the stability analysis, made in the Appendix, Sec. 1. We get again a pair of complex roots with the real part very close to zero, both with and without an injected signal. Their imaginary parts are of the order of unity for $r = 10^2$, thus spoiling squeezing in the region $\tilde{\omega} \approx 1$. For higher pumping rates the peaks are pulled to higher frequencies such that, for $r = 10^4$ and $x = 0.85$, which correspond to the solid curve in Fig. 5(b), the absolute value of the imaginary parts of the roots is $\tilde{\omega} \sim 8$ and, for $r = 10^6$ [Fig. 5(c)], $\tilde{\omega} \sim 80$.

V. CONCLUSION

We have shown, through a detailed analysis which does not involve the adiabatic elimination of field or

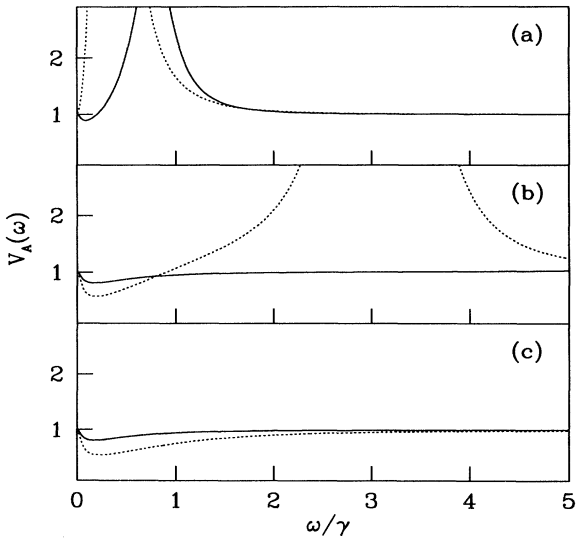

FIG. 5. Normalized spectra of amplitude fluctuations for the fourth class of lasers with Poissonian pumping statistics and $a = 10^{-3}$, $b = 10^{-1}$, and $c = 0.5$. The dotted line corresponds to no signal injected and the solid line corresponds to $x = 0.85$. (a) $r = 10^2$, (b) $r = 10^4$, and (c) $r = 10^6$.

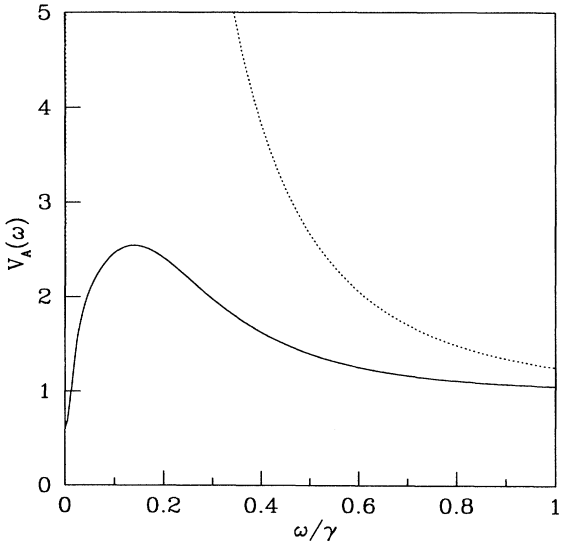

FIG. 6. Normalized spectra of amplitude fluctuations for the fourth class of lasers with regular pumping statistics ($p = 1$) and $a = 10^{-3}$, $b = 10^{-1}$, and $c = 0.5$. The pumping parameter is $r = 3$. The dotted line corresponds to no signal injected and the solid line corresponds to $x = 0.85$.

atomic variables, that an injected signal helps to improve both amplitude squeezing and sub-shot-noise behavior for lasers operating close to threshold, spoiling noise reduction, however, for high pumping rates. Several cases have been analyzed so as to cover all laser families. The noise increase in some cases is related to the proximity of instability thresholds. Regularization of the pumping helps to get sub-Poissonian light, which can, however, also be obtained for Poissonian pumping, in the situation when the polarization can be adiabatically eliminated, and the laser is described by rate equations. In this case, injection of an external signal helps to reduce the pumping necessary for noise compression to be obtained.

ACKNOWLEDGMENTS

This work was partially supported by the Brazilian Agencies Conselho Nacional de Desenvolvimento Científico e Tecnológico, Coordenação de Aperfeiçoamento do Pessoal de Ensino Superior, and Secretaria de Ciência e Tecnologia.

APPENDIX: STABILITY ANALYSIS

1. General case

We analyze here the stability of the steady-state solutions for the laser with an injected signal. In order to simplify the analysis, we write the dynamic equations for c-number variables, Eqs. (16), in terms of their corresponding amplitudes and phases. So we define

$$\mathcal{A} \equiv \rho e^{i\phi}, \quad \mathcal{M} \equiv m e^{i\theta},$$

getting the equations

$$\dot{\rho}(t) = gm(t)\cos[\theta(t)-\phi(t)] - \tfrac{\gamma}{2}\rho(t) + \tfrac{\gamma}{2}\lambda\cos\phi(t), \tag{A1}$$

$$\dot{m}(t) = -\Gamma m(t) + g[\mathcal{N}_a(t)-\mathcal{N}_b(t)]\rho(t)\cos[\theta(t)-\phi(t)], \tag{A2}$$

$$\dot{\mathcal{N}}_a(t) = R - (\Gamma_a+\Gamma'_a)\mathcal{N}_a(t) - 2gm(t)\rho(t)\cos[\theta(t)-\phi(t)], \tag{A3}$$

$$\dot{\mathcal{N}}_b(t) = -\Gamma_b\mathcal{N}_b(t) + \Gamma'_a\mathcal{N}_a(t) + 2gm(t)\rho(t)\cos[\theta(t)-\phi(t)] \tag{A4}$$

for the amplitudes and

$$\dot{\phi}(t) = \frac{gm(t)}{\rho(t)}\sin[\theta(t)-\phi(t)] - \frac{\gamma}{2}\frac{\lambda}{\rho(t)}\sin\phi(t), \tag{A5}$$

$$\dot{\theta}(t) = -\frac{g\rho(t)}{m(t)}[\mathcal{N}_a(t)-\mathcal{N}_b(t)]\sin[\theta(t)-\phi(t)] \tag{A6}$$

for the phases. Notice that, in the above equations, we have chosen $\beta = 0$ for the injected signal phase, that is, λ is real and positive. This choice is of course irrelevant and our results can be easily generalized to complex inputs.

The steady-state solutions corresponding to Eqs. (A5) and (A6) are $\phi_s = n\pi$ and $\theta_s = (n+l)\pi$, where n and l are integers. Their stability can be easily checked from the drift matrix, obtained by linearizing Eqs. (A5) and (A6) around the steady state,

$$\begin{pmatrix} -\frac{\gamma}{2} & \frac{\gamma}{2}(1-\frac{\lambda}{\rho_s}\cos\phi_s) \\ \Gamma & -\Gamma \end{pmatrix}.$$

The above matrix has eigenvalues

$$\alpha_+ = -\frac{\mu}{2}+\nu, \quad \alpha_- = -\frac{\mu}{2}-\nu,$$

where

$$\mu \equiv (\Gamma+\tfrac{\gamma}{2}), \quad \nu \equiv \sqrt{\tfrac{1}{4}\mu^2 - \tfrac{\gamma\Gamma}{2}\frac{\lambda}{\rho_s}\cos\phi_s}\,.$$

Inspection of the eigenvalues α_+ and α_- shows that both have a negative real part, indicating a stable steady state, if and only if $\cos\phi_s > 0$. This means that the stable steady phase is $\phi_s = 0 \pmod{2\pi}$, for a real positive injected signal, or, better, the ratio $\lambda/\mathcal{A}_s$ is always positive.

We are now able to check the stability of the steady-state amplitudes. In order to shorten the notation, we define $u_s \equiv \cos(\theta_s - \phi_s)$. Linearizing Eqs. (A1) – (A4) one gets the drift matrix

$$D = \begin{pmatrix} -\gamma/2 & gu_s & 0 & 0 \\ \frac{\Gamma\gamma}{2g}(1-\frac{\lambda}{\rho_s})u_s & -\Gamma & g\rho_s u_s & -g\rho_s u_s \\ -\gamma\rho_s(1-\frac{\lambda}{\rho_s}) & -2g\rho_s u_s & -(\Gamma_a+\Gamma'_a) & 0 \\ \gamma\rho_s(1-\frac{\lambda}{\rho_s}) & 2g\rho_s u_s & \Gamma'_a & -\Gamma_b \end{pmatrix}, \tag{A7}$$

whose eigenvalues are the roots of the characteristic polynomial

$$f(y) = c_0 y^4 + c_1 y^3 + c_2 y^2 + c_3 y + c_4\,. \tag{A8}$$

The coefficients c_j, written in terms of the dimensionless parameters a, a', b, c, r, and x, as defined in Eq. (39), are

$$\begin{aligned} c_0 &= 1, \\ c_1 &= a + a' + b + c + \tfrac{1}{2}, \\ c_2 &= b(a+a') + (a+a'+b)(\tfrac{1}{2}+c) + 2cb\frac{(a+a')}{(a+b)}\left[\frac{r}{1-x}-1\right] + \frac{c}{2}x, \\ c_3 &= b(a+a')(\tfrac{1}{2}+c) + \frac{c}{2}(a+a'+b)x + cb(a+a')\left[\frac{r}{1-x}-1\right] \\ &\quad + cb\frac{(a+a')}{(a+b)}(2-x)\left[\frac{r}{1-x}-1\right], \\ c_4 &= \frac{cb}{2}(a+a')\left[\frac{r(2-x)}{1-x} - 2(1-x)\right]. \end{aligned}$$

Since the coefficients c_j do not depend on $u_s \equiv \cos(\theta_s - \phi_s)$, we conclude that the steady-state atomic polarization phase $\theta_s = \phi_s + l\pi$, for any l integer, is always stable.

In order to avoid finding the roots of (A8), we use, at this point, the *Hurwitz criterion* [19], which allows

us to check, directly from the properties of the matrix D, whether $\mathrm{Re}(y) < 0$. According to that criterion, the roots of the polynomial (A8) have a negative real part if and only if the following conditions are fulfilled:

$$\frac{c_1}{c_0} > 0, \frac{c_2}{c_0} > 0, \ldots, \frac{c_4}{c_0} > 0$$

and the principal subdeterminants H_j (Hurwitz determinants) of the quadratic scheme

$$\begin{matrix} c_1 & c_0 & 0 & 0 \\ c_3 & c_2 & c_1 & c_0 \\ 0 & c_4 & c_3 & c_2 \\ 0 & 0 & 0 & c_4 \end{matrix}$$

satisfy the inequalities $H_1 > 0$, $H_2 > 0$, ..., $H_4 > 0$.

For a degree-four polynomial, the Hurwitz determinants read as

$$H_1 = c_1, \quad H_2 = c_1c_2 - c_0c_3,$$
$$H_3 = c_3H_2 - c_1^2c_4, \quad H_4 = c_4H_3 .$$

It is easy to see that the first Hurwitz condition is satisfied for any positive x, which is the region we are interested in, since the phase analysis showed us already that steady-state solutions with negative x are unstable. We are left with the second Hurwitz condition. But, since H_1 is clearly positive and H_4 is positive unless H_3 is not, we only have to examine H_2 and H_3. For simplicity, we set $a' = 0$. After some algebra we get the following expressions:

$$H_2 = abc\left[\frac{1}{1-x} - \frac{1}{a+b} + \frac{2c}{(a+b)(1-x)}\right]r + \frac{c(1+2c)}{4}\frac{x}{1-x}$$
$$+\frac{abc}{(a+b)}(1-x) + \frac{(a+b)}{4}(1+2a+2b) + a(a+b)(b+c) + (a+b)c + b^2c + c^2\frac{(a^2+b^2)}{(a+b)}, \tag{A9}$$

$$H_3 = \frac{a^2b^2c^2r^2}{(a+b)^2(1-x)^2}[(1-x)(2c-1) - (1-x)^2 + (a+b+1)(a+b+2c)]$$
$$+\frac{abcr}{8(a+b)^2(1-x)}(2c(1-x)^2[(a+b)(2a+2b-2c-1) + 8ab]$$
$$+(1-x)\{[(a+b)^2[(1+2c)(1-4c) - 4(a^2+b^2)] - 4(a+b)^3c - 4ab(a+b)(1+2c) + 16abc(1-2c)]\}$$
$$+\{2(a+b)^3[4(a+c)(b+c) + (1+6c)] + (a+b)^2[1+6c+ab(12-c)]$$
$$+2(a+b)c[1+2c-ab(4+c)] + 16(a^2+b^2)c^2\})$$
$$+\frac{1}{8(a+b)^2}(c^2(1-x)^2\{[(a+b)^2+2ab][(a+b)(1+2c) - 4ab]\}$$
$$+(1-x)\{-1(a+b)^5(1+2c) - (a+b)^4[(1+2c)^2 - 4ab] + (a+b)^3[(1+2c)(4ab-2c) + 4abc]$$
$$+ab(a+b)^2[(2c-1) + 8(c^2-ab)] + 4a^2b^2[a+b+2c(2c-1)]\}$$
$$+\{2c(a+b)^5(1+2c) + (a+b)^4(1+4c)(2ab+c) + (a+b)^3[c^2(2c+1) + ab(1+4ab-8c^2)]$$
$$-abc(a+b)^2(1+12ab+6c) - 2abc^2(a+b)(1+2c) + 4(a^2+b^2)^2c^3\}). \tag{A10}$$

The above expressions are too big for a full analysis. However, we can examine them in some special regions of parameters. The following two regions are particularly interesting for our purposes, since they lead to squeezing.

a. Far above threshold ($r \gg 1$)

In this case, Eqs. (A9) and (A10) reduce to

$$H_2 = abc\frac{r}{1-x}\left[1 + \frac{2c}{(a+b)} - \frac{(1-x)}{(a+b)}\right], \tag{A11}$$

$$H_3 = \frac{a^2b^2c^2}{(a+b)^2}\frac{r^2}{(1-x)^2}\left[(1-x)(2c-1) - (1-x)^2 + (a+b+1)(a+b+2c)\right]. \tag{A12}$$

Both expressions Eqs. (A11) and (A12) become negative, implying an unstable steady state, when

$$(1-x) > a+b+2c.$$

Otherwise, the steady state is stable. This will be the case whenever one of the constants a, b, or c becomes much larger than unity, implying that the first three classes of lasers are always stable, far above threshold. This does not necessarily hold, however, for the fourth class. The parameters involved in the analysis presented in Sec. IV C were chosen, however, so that H_2 and H_3 above are positive.

b. Strong injected signal

One can easily see that setting $(1-x) \ll 1$ while keeping $r \sim 1$ in Eqs. (A9) and (A10) produces

$$H_2 = abc\frac{r}{1-x}\left[1 + \frac{2c}{(a+b)}\right] + \frac{c(1+2c)}{4}\frac{x}{1-x}, \tag{A13}$$

$$H_3 = \frac{a^2b^2c^2}{(a+b)^2}\frac{r^2}{(1-x)^2}(a+b+1)(a+b+2c), \tag{A14}$$

which are positive for any value of a, b and c, indicating stability.

2. Second and third classes of lasers

In this case, the atomic polarization can be adiabatically eliminated, hence the dynamic equations for the c-number variables become

$$\dot{\mathcal{A}}(t) = \frac{g^2}{\Gamma}\left[\mathcal{N}_a(t) - \mathcal{N}_b(t)\right]\mathcal{A}(t) - \frac{\gamma}{2}\mathcal{A}(t) + \frac{\gamma}{2}\lambda, \quad \text{(A15)}$$

$$\dot{\mathcal{N}}_a(t) = R - \frac{2g^2}{\Gamma}\left[\mathcal{N}_a(t) - \mathcal{N}_b(t)\right]|\mathcal{A}(t)|^2 - (\Gamma_a + \Gamma'_a)\mathcal{N}_a(t), \quad \text{(A16)}$$

$$\dot{\mathcal{N}}_b(t) = \frac{2g^2}{\Gamma}\left[\mathcal{N}_a(t) - \mathcal{N}_b(t)\right]|\mathcal{A}(t)|^2 - \Gamma_b\mathcal{N}_b(t) + \Gamma'_a\mathcal{N}_a(t). \quad \text{(A17)}$$

Linearization of the above equations around steady state leads to a 3×3 drift matrix whose characteristic polynomial

$$f(y) = c_0y^3 + c_1y^2 + c_2y + c_3$$

has coefficients

$$c_0 = 1,$$

$$c_1 = \frac{2(a^2+b^2)(1-x) + (a+b)(1-x)x + 4abr}{2(a+b)(1-x)},$$

$$c_2 = \frac{2ab(a+b)r + 2ab(x+r-1) + (a+b)^2(1-x)x}{2(a+b)(1-x)},$$

$$c_3 = \frac{ab\left[r-(1-x)^2\right]}{2(1-x)},$$

where we have again set $\Gamma'_a = 0$ in order to simplify the analysis.

One can easily see that the coefficients c_0, c_1, c_2, and c_3 are positive for any x positive. So the first Hurwitz condition is fulfilled. On the other hand, the second Hurwitz condition for a third-degree polynomial reads as

$$H_1 = c_1 > 0, \quad H_2 = c_1c_2 - c_0c_3 > 0, \quad H_3 = c_3H_2 > 0.$$

Thus instability may only come from the second Hurwitz subdeterminant

$$H_2 = \frac{1}{4(a+b)^2(1-x)^2}\{2(a^4+b^4)(1-x)^2x + 4a^2b^2\left[(a-x)^2+2r^2\right] + 8ab(a^2+b^2)(1-x)r + (a^3+b^3)(1-x)^2x^2 + ab(a+b)(1-x)x\left[2r+(1-x)\right] + 4ab(a^3+b^3)(1-x)r + 4a^2b^2(a+b)(1-x+2r)r - 6ab(a+b)^2(1-x)^2r - 2ab(a^2+b^2)(1-x)^3 - 3ab(a+b)(1-x)^3x\}. \quad \text{(A18)}$$

We analyze first two limit cases, which will be useful for the discussion of the general situation.

a. Far above threshold

By setting $r \gg 1$ in expression (A18) we get

$$H_2 = \frac{2a^2b^2(a+b+1)}{(a+b)^2(1-x)^2}r^2,$$

which is clearly positive, indicating stability.

b. For all x with r = 1

In this case, Eq. (A18) reduces to

$$H_2 = \frac{1}{4(a+b)^2(1-x)}\{4ab(a^2+b^2)(a+b) + 2(a^4+b^4)(1-x)x + 2ab(a^2+b^2)(5-x)x + (a^3+b^3)(1-x)x + ab(a+b)(5-3x)x^2\} + \frac{2a^2b^2}{(a+b)^2(1-x)^2}\left[1+a+b-(1-x)^2\right]. \quad \text{(A19)}$$

Simple inspection of the above expression shows that H_2 is positive also for $r = 1$. These two special cases allow us now to consider the general situation. Since H_2 is positive for both $r \gg 1$ and $r = 1$, there is just one possibility for a change of signal at an intermediate r: a negative minimum in this region. The only minimum of H_2 occurs at

$$r_0 = \frac{(1-x)}{(1+a+b)} - \frac{(1-x)(a+b)}{8ab(1+a+b)}[(a+b)(1+3x) + 2(a^2+b^2) + x], \quad \text{(A20)}$$

which is below threshold ($r = 1$). We conclude that H_2 stays positive for all values of $r \geq 1$. Therefore, the second and third classes of lasers are always stable.

[1] Y. M. Golubev and I. V. Sokolov, Zh. Eksp. Teor. Fiz. **87**, 408 (1984) [Sov. Phys. JETP **60**, 234 (1984)]; M. C. Teich and B. E. A. Saleh, J. Opt. Soc. Am. B **2**, 275 (1985); Y. Yamamoto, S. Machida, and O. Nilsson, Phys. Rev. A **34**, 4025 (1986); S. Machida, Y. Yamamoto, and Y. Itaya, Phys. Rev. Lett. **58**, 1000 (1987); Y. Yamamoto and S. Machida, Phys. Rev. A **35**, 5114 (1987); M. A. Marte, H. Ritsch, and D. F. Walls, Phys. Rev. Lett. **61**, 1093 (1988); J. Bergou, L. Davidovich, M. Orszag, C. Benkert, M. Hillery, and M. O. Scully, Opt. Commun. **72**, 82 (1989); J. Bergou, L. Davidovich, M. Orszag, C. Benkert, M. Hillery, and M. O. Scully, Phys. Rev. A **40**, 5073 (1989); T. A. B. Kennedy and D. F. Walls, *ibid.* **40**, 6366 (1989); F. Haake, S. M. Tan, and D. F. Walls, *ibid.* **40**, 7121 (1989); A. M. Khazanov, G. A. Koganov, and E. P. Gordov, *ibid.* **42**, 3065 (1990); T. C. Ralph and C. M. Savage, Opt. Lett. **16**, 1113 (1991); D. L. Hart and T. A. B. Kennedy, Phys. Rev. A **44**, 4572 (1991).

[2] C. Benkert, M. O. Scully, J. Bergou, L. Davidovich, M. Hillery, and M. Orszag, Phys. Rev. A **41**, 2756 (1990).

[3] M. O. Scully, Phys. Rev. Lett. **55**, 2802 (1985); M. O. Scully and M. S. Zubairy, Phys. Rev. A **35**, 752 (1987); J. Bergou, M. Orszag, and M. O. Scully, *ibid.* **38**, 768 (1988); J. Krause and M. O. Scully, *ibid.* **36**, 1771 (1987); M. O. Scully, K. Wódkiewicz, M. S. Zubairy, J. Bergou, N. Lu, and J. Meyer-ter-Vehn, Phys. Rev. Lett. **60**, 1832 (1988); C. Benkert, M. O. Scully, and M. Orszag, Phys. Rev. A **42**, 1487 (1990); for experimental results see M. Winters, J. Hall, and P. Toschek, Phys. Rev. Lett. **65**, 3116 (1990).

[4] J. Bergou, C. Benkert, L. Davidovich, M. O. Scully, S.-Y. Zhu, and M. S. Zubairy, Phys. Rev. A **42**, 5544 (1990); S. M. Dutra and L. Davidovich, *ibid.* **49**, 2986 (1994).

[5] H. Ritsch, P. Zoller, C. W. Gardiner, and D. F. Walls, Phys. Rev. A **44**, 3361 (1991).

[6] M. Kolobov, L. Davidovich, E. Giacobino, and C. Fabre, Phys. Rev. A **47**, 1431 (1993).

[7] M. B. Spencer and W. E. Lamb, Jr., Phys. Rev. A **5**, 884 (1975).

[8] T. Yamada and R. Graham, Phys. Lett. **53A**, 77 (1975); L. A. Lugiato, Lett. Nuovo Cimento **23**, 609 (1978); H. J. Scholz, T. Yamada, H. Brand, and R. Graham, Phys. Lett. **82A**, 321 (1981); L. A. Lugiato, L. M. Narducci, D. K. Bandy, and C. A. Pennise, Opt. Commun. **46**, 64 (1983); F. T. Arecchi, G. L. Lippi, G. P. Puccioni, and J. R. Tredicce, *ibid.* **51**, 308 (1984); G. L. Oppo and A. Politi, Z. Phys. B **59**, 111 (1985); Y. Gu, D. K. Bandy, J. M. Yuan, and L. M. Narducci, Phys. Rev. A **31**, 354 (1985); D. K. Bandy, L. M. Narducci, and L. A. Lugiato, J. Opt. Soc. Am. B **2**, 148 (1985); J. R. Tredicce, F. T. Arecchi, G. L. Lippi, and G. P. Puccioni, *ibid.* **2**, 173 (1985); A. Politi, G. L. Oppo, and R. Badii, Phys. Rev. A **33**, 4055 (1986); G. L. Oppo, A. Politi, G. L. Lippi, and F. T. Arecchi, *ibid.* **34**, 4000 (1986); R. Holzner, B. Derighetti, M. Ravani, and E. Brun, *ibid.* **36**, 1280 (1987); Hu Gang and Yang Guo-jian, *ibid.* **38**, 1979 (1988); A. Baugher, P. Hammack, and J. Lin, *ibid.* **39**, 1549 (1989); Hu Gang and Yang Guo-jian, *ibid.* **40**, 834 (1989); D. J. Jones and D. K. Bandy, J. Opt. Soc. Am. B **7**, 2119 (1990); P. A. Braza and Th. Erneux, Phys. Rev. A **41**, 6470 (1990); H. Zeghlache and V. Zehnlé, *ibid.* **46**, 6015 (1992); V. Zehnlé and H. Zeghlache, *ibid.* **46**, 6030 (1992).

[9] M. Lax, Phys. Rev. **145**, 110 (1966); also in *Physics of Quantum Electronics,* edited by P. L. Kelley, B. Lax, and P. E. Tannenwald (McGraw-Hill, New York, 1966), p. 735.

[10] See, for instance, W. H. Louisell, *Quantum Statistical Properties of Radiation* (Wiley, New York, 1973); M. Sargent III, M. O. Scully, and W. E. Lamb, Jr., *Laser Physics* (Addison Wesley, Reading, MA, 1974); C. Cohen-Tannoudji, J. Dupont-Roc, and G. Grynberg, *Processus d'Interaction entre Photons et Atomes* (InterEditions/Editions du CNRS, Paris, 1988); M. Lax, in *Statistical Physics, Phase Transitions and Superconductivity,* edited by M. Chrétien, E. P. Gross, and S. Dreser (Gordon and Breach, New York, 1968), Vol. II, p. 425.

[11] B. R. Mollow, Phys. Rev. **188**, 1969 (1969).

[12] M. D. Reid, Phys. Rev. A **37**, 4792 (1988).

[13] M. J. Collet and C. W. Gardiner, Phys. Rev. A **30**, 1386 (1984); C. M. Caves and B. L. Schumaker, *ibid.* **31**, 3068 (1985); B. L. Schumaker and C. M. Caves, *ibid.* **31**, 3093 (1985); C. W. Gardiner and M. J. Collet, *ibid.* **31**, 3761 (1985); M. J. Collet and D. F. Walls, *ibid.* **32**, 2887 (1985).

[14] N. A. Abraham, P. Mandel, and L. M. Narducci, in *Dynamic Instabilities and Pulsations in Lasers*, edited by E. Wolf, Progress in Optics XXV (Elsevier, Amsterdam, 1986).

[15] G. S. Agarwal, J. A. Bergou, C. Benkert, and M. O. Scully, Phys. Rev. A **43**, 6451 (1991).

[16] F. A. M. de Oliveira and P. L. Knight, Phys. Rev. A **39**, 3417 (1989).

[17] D. Stoler, Phys. Rev. D **1**, 3217 (1970); **4**, 1925 (1971); H. P. Yuen, Phys. Rev. A **13**, 2226 (1976).

[18] W. Schleich and J. A. Wheeler, J. Opt. Soc. Am. B **4**, 1715 (1987).

[19] H. Haken, *Synergetics: An Introduction*, 3rd ed. (Springer, Heidelberg, 1983).